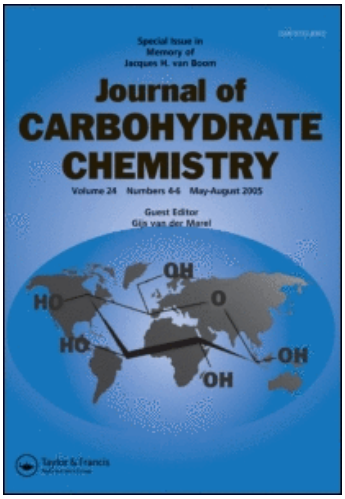

Journal of Carbohydrate Chemistry

Publication details, including instructions for authors and subscription information:
http://www.informaworld.com/smpp/title~content=t713617200

NMR and Monte Carlo Studies on the Solution Conformation of a Linear Capsular Polysaccharide from a Soybean-Nodulating Bacterium (Strain B33)

Miguel A. Rodríguez-Carvajal[ab]; Antonio M. Gil-Serrano[a]; Pilar Tejero-Mateo[a]; José L. Espartero[c]; Serge Pérez[b]

[a] Departamento de Química Orgánica, Facultad de Química, Universidad de Sevilla, Sevilla, Spain [b] CNRS, Centre de Recherches sur les Macromolécules Végétales, Grenoble, France [c] Departamento de Química Orgánica y Farmacéutica, Facultad de Farmacia, Universidad de Sevilla, Sevilla, Spain

Online publication date: 12 November 2003

To cite this Article Rodríguez-Carvajal, Miguel A. , Gil-Serrano, Antonio M. , Tejero-Mateo, Pilar , Espartero, José L. and Pérez, Serge(2003) 'NMR and Monte Carlo Studies on the Solution Conformation of a Linear Capsular Polysaccharide from a Soybean-Nodulating Bacterium (Strain B33) ', Journal of Carbohydrate Chemistry, 22: 7, 765 — 779

To link to this Article: DOI: 10.1081/CAR-120026474

URL: http://dx.doi.org/10.1081/CAR-120026474

JOURNAL OF CARBOHYDRATE CHEMISTRY
Vol. 22, Nos. 7 & 8, pp. 765–779, 2003

NMR and Monte Carlo Studies on the Solution Conformation of a Linear Capsular Polysaccharide from a Soybean-Nodulating Bacterium (Strain B33)†

Miguel A. Rodríguez-Carvajal,[1,3] Antonio M. Gil-Serrano,[1] Pilar Tejero-Mateo,[1] José L. Espartero,[2] and Serge Pérez[3,*]

[1]Departamento de Química Orgánica, Facultad de Química and
[2]Departamento de Química Orgánica y Farmacéutica, Facultad de Farmacia,
Universidad de Sevilla, Sevilla, Spain
[3]Centre de Recherches sur les Macromolécules Végétales,
Grenoble, France

ABSTRACT

The conformational behavior of the capsular polysaccharide obtained from a fast-growing soybean-nodulating *rhizobia* (strain B33) isolated from Xinjiang Autonomous Region (Eastern China) has been analyzed by NMR and molecular mechanics simulations. This polysaccharide has the repeating unit →6)-4-*O*-Me-α-D-Glc*p*-(1 → 4)-3-*O*-Me-β-D-Glc*p*A-(1→. The NMR results indicate that the α-(1 → 4) linkage may adopt a variety of conformations, and that at least two of the resulting minima must exist in solution. NOE data agree with an 85:10:5 ratio for the lowest-energy conformations. In the case of the β-(1 → 6) linkage, NMR indicates that the rotamer *gg* is highly populated. Experimental and calculated NOE intensities match well when the global energy minimum conformation for this linkage has exclusively the *gg* orientation. The influence of the adjacent methyl group on the glycosyloxymethyl population has been evaluated by simulation of a disaccharide without this

†This paper is dedicated to Professor Gérard Descotes on the occasion of his 70th birthday.
*Correspondence: Serge Pérez, Centre de Recherches sur les Macromolécules Végetáles, BP 53, 38041 Grenoble, France; Fax: 33-476-03-76-29; E-mail: perez@cermav.cnrs.fr.

DOI: 10.1081/CAR-120026474
0732-8303 (Print); 1532-2327 (Online)
www.dekker.com

MARCEL DEKKER, INC.
270 Madison Avenue, New York, New York 10016

group. A relative destabilization of *gt* rotamer has been found. Long chains have been simulated using a Metropolis algorithm at different ratios of the *gg* and *gt* rotamers in the glucose moiety. It was observed that the increase in population of the *gt* rotamer yielded more close contacts in the chain.

Key Words: Root nodule synbiose; Capsular polysaccharide; Structure; Nuclear magnetic resonance; Molecular modeling.

INTRODUCTION

Five of the seven genera composing the bacterial family *Rhizobiaceae* are able to form root–nodule symbioses with members of the plant family *Leguminosae*:[1] *Rhizobium*, *Bradyrhizobium*, *Sinorhizobium*, *Mesorhizobium*, and *Azorhizobium*. Nodules are unique plant organs in which bacteria are differentiated into bacteroids, and fix atmospheric nitrogen. The *Rhizobium*–plant interaction is host specific and determined by exchange of chemical signals between the two partners.[2] Although it is known that the development of nodules is induced by bacterial Nod factors (lipo–chito–oligosaccharides), additional signals—such as those from bacterial surface polysaccharides—are required for the invasion of the plant cells by rhizobia, and the subsequent formation of nitrogen-fixing nodules.[3,4] These polysaccharides, named exopolysaccharides (EPS), lipopolysaccharides (LPS), capsular polysaccharides (KPS), and cyclic glucans, are the main carbohydrate components of the bacterial surface. Although their exact function has not been clearly established, they appear to play important roles in the ability of the bacteria to invade the root and to avoid the triggering of plant-defenses, as well as in cell–cell communication.[3,4]

In a recent publication,[5] we reported the primary structure of a K-antigen isolated from a fast-growing soybean-nodulating rhizobia (strain B33) found in Xinjiang Autonomous Region (Eastern China), belonging most probably to either the species *Sinorhizobium fredii* or the species *Sinorhizobium xinjiangense*. This strain is able to form nitrogen-fixing nodules on both Asiatic and American soybean cultivars. Its capsular polysaccharide (**1**) has a repeating unit consisting of the disaccharide →6)-4-*O*-Me-α-D-Glc*p*-(1 → 4)-3-*O*-Me-β-D-Glc*p*A-(1→. We now report on the study of the solution conformation of the K-antigen isolated from strain B33, using NMR techniques and molecular modeling.[6,7] The orientations around the glycosidic linkages have been analyzed.

EXPERIMENTAL PROCEDURES

Molecular Modeling Calculations

A representation of the repeating unit of the K-antigen is given in Figure 1, along with the labeling of the torsion angles of interest. For the sake of simplicity, the 3-*O*-methyl-β-D-glucuronic acid (3-*O*-Me-β-D-Glc*p*A) is abbreviated as (A), and the 4-*O*-methyl-α-D-glucopyranose unit (4-*O*-Me-α-D-Glc*p*) as (B). The conformations around the glycosidic linkages are described by two sets of torsion angles: Φ_A = O5(A)–C1(A)–O1(A)–C6(B), Ψ_A = C1(A)–O1(A)–C6(B)–C5(B) (A → B linkage) and

Marcel Dekker, Inc.
270 Madison Avenue, New York, New York 10016

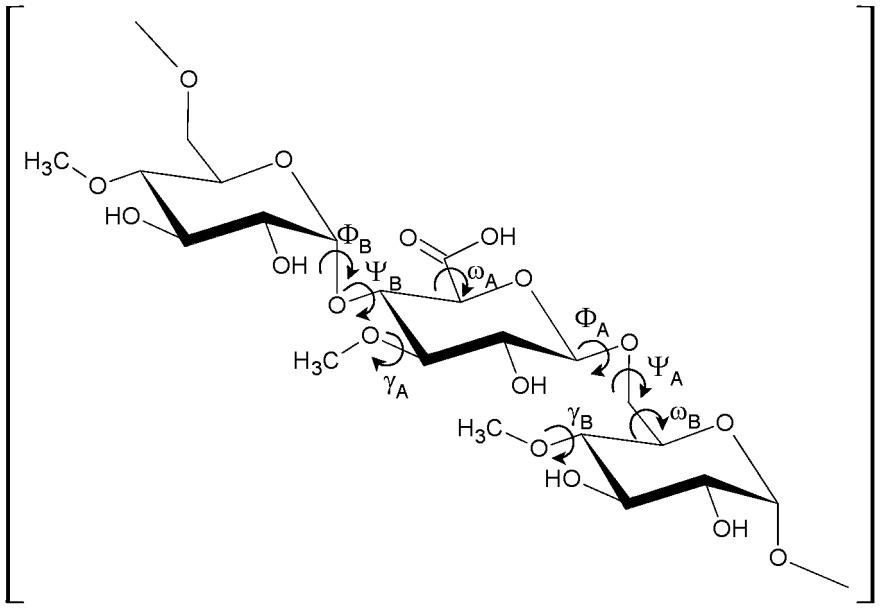

Figure 1. Representation of the repeating unit of the K-antigen isolated from strain B33. Studied torsion angles are also indicated.

Φ_B = O5(B)–C1(B)–O1(B)–C4(A), Ψ_B = C1(B)–O1(B)–C4(A)–C3(A) (B → A linkage). For the description of the β-(1 → 6) linkage, a torsion angle describing the glycosyloxymethyl orientation in residue B must be included: ω_B = O5(B)–C5(B)–C6(B)–O1(A). Other important torsion angles considered in the study are those describing the orientation of the methyl groups in residues A and B, as well as that of the acid moiety in residue A. They are defined as

$$\gamma_A = C2(A)—C3(A)—O3(A)—C'3(A)$$

$$\gamma_B = C3(B)—C4(B)—O4(B)—C'4(B)$$

and

$$\omega_A = O5(A)—C5(A)—C6(A)—OH(A)$$

respectively.

The signs of the torsion angles are in agreement with the IUPAC-IUB commission of Biochemical Nomenclature.[8]

The general molecular mechanics program MM3(92)[9–11] was used in this study to compute the energy of di- or oligosaccharide conformations, using a dielectric constant ε = 80 to simulate water. Polysaccharide conformations depend mainly on the Φ and Ψ glycosidic torsion angles and can, as a first approximation, be described by the (Φ,Ψ) potential energy maps of the disaccharide subunits. Following this assumption, adiabatic maps were computed for the AB and BA disaccharides. Previous

studies have shown that the carbonyl oxygen and the acid proton preferentially adopt a *trans* orientation.[12] The ω_A torsion angle exhibits two main orientations, with 130–140° being the more favorable. The latter was selected for the carboxyl group in all the disaccharides. Only the *gg* ($\omega_B \sim 300°$) and *gt* ($\omega_B \sim 60°$) orientations were considered for ω_B, as they are the most-populated experimentally.[13,14] The orientations of the secondary hydroxyl groups were set either clockwise (*c*) or counter-clockwise (*r*) in both monomers, and combined with ω_B rotamers to generate eight possible starting structures for each adiabatic map. The relaxed maps were computed using rigid rotation in 10° intervals for Φ and Ψ spanning the whole angular range, followed by minimization using the block diagonal method with a termination criterion of n*0.00003 kcal/mol (n: number of atoms). Finally, the adiabatic map was constructed for each disaccharide, using the lowest-energy conformation from the relaxed maps for each grid point. The isoenergy contour maps were drawn using the program Xfarbe.[15]

Molecular mechanics calculations were also performed with the CICADA (Channels in Conformational Space Analyzed by Driver Approach) algorithm for conformational searches.[16] This method explores the potential energy surface by driving each selected torsion angle separately, with a full-geometry optimization at each increment (except for the driven angle). Thus, it concentrates mostly on the exploration of the low-energy regions of the potential energy surface, saving a significant amount of computational time and allowing the inclusion of more variables in the study.

In order to evaluate the behavior of the polysaccharide chains in solution, large ensembles of disordered chains were generated using the Monte Carlo technique as implemented in the METROPOL program.[17] Experimental conditions can be selected so that there are no interactions between non-neighboring monomers. These conditions (called theta-conditions) are simulated with the program METROPOL, which is based on the Metropolis algorithm.[18] A detailed description of the procedure has been reported elsewhere.[17] Using this approach, statistical ensembles (at 298 K) of 10000 polymer chains, each containing 5000 residues, were constructed for **1**. The extension and relative stiffness of the chain can be described by the persistence length (L_p),[19] which is defined as the projection of the end-to-end distance vector r on the first bond of the chain. It represents the maximum length over which a straight direction is preserved. L_p increases asymptotically with the degree of polymerization, achieving a value where it becomes independent. No long-range interactions between residues are considered in this kind of calculation.

NMR Spectroscopy

Samples were deuterium-exchanged several times by freeze drying from D_2O, and then analyzed in solution (4 mg/mL) in 99.98% D_2O. Spectra were recorded at 303 K on a Bruker AMX500 spectrometer operating at 500.13 MHz (^{1}H) and 125.75 MHz (^{13}C). Chemical shifts are given in ppm, using the HDO signal (4.75 ppm) (^{1}H) and external dimethylsulfoxide (39.5 ppm) (^{13}C) as references. The 2D homonuclear COSY was performed using the Bruker standard pulse sequence. The 2D heteronuclear one-bond proton–carbon correlation experiment was registered in the ^{1}H-detection mode via single-quantum coherence (HSQC). A data matrix of 256*1K points was used to digitize a spectral width of 3000 and 26000 Hz in F_2 and F_1; 64 scans were used per

Marcel Dekker, Inc.
270 Madison Avenue, New York, New York 10016

increment, with a delay between scans of 1 s and a delay corresponding to a $^{1}J_{H,C}$ value of 150 Hz. ^{13}C decoupling was achieved by the GARP scheme. Squared sine-bell functions were applied in both dimensions, and zero-filling was used to expand the data to 512*1K. This experiment was slightly modified by the implementation of an editing block in the sequence.[20] The HMBC experiment was performed using the Bruker standard sequence with 256 increments of 2K real points to digitize a spectral width of 3000*28000 Hz. 192 scans were acquired per increment with a delay of 50 ms for evolution of long-range couplings. The pure absorption 2D NOESY[21] experiments were performed with mixing times of 50, 100, 200, and 300 ms. A data matrix of 256*1K points was used to digitize a spectral width of 3000 Hz; 96 scans were used per increment with a delay between scans of 1 s. Squared sine-bell functions were applied in both dimensions, and zero-filling was used to expand the data to 1K*2K. Good linearity was observed up to 200 ms in all signals except for $H6_S$(B)/$H6_R$(B). Assignment and integration of spectra were performed using the program SPARKY.[22] The NOESY intensities were calculated according to the complete relaxation matrix,[23] using the program NOEPROM.[24] Isotropic motion and external relaxation of 0.1 s^{-1} were assumed in the calculation.[24] Since NOEs are dependent on the correlation time (τ_c), different values were used in order to obtain the best match between experimental and calculated NOEs for the H1(A)/H5(A) and H1(B)/H2(B) pairs.

RESULTS

Nuclear Magnetic Resonance

Since NMR parameters are time-averaged, the information that may be deduced from these experiments corresponds to the time-averaged conformation in solution.

^{1}H NMR and ^{13}C NMR spectra of the capsular polysaccharide B33 were completely assigned by a combination of homonuclear (COSY, TOCSY) and heteronuclear (HSQC, HMBC) techniques. The corresponding ^{1}H NMR chemical shifts, as well as the $^{3}J_{H,H}$, are listed in Tables 1 and 2. The assignment of the C-6 protons in residue B was based on the work of Nishida et al.[25,26] Those authors found that, for a β-(1 → 6) linkage, the pro-*S* hydrogen is more deshielded than its partner. The NOEs found between the proton

Table 1. ^{1}H NMR chemical shifts (δ, ppm) for **1**.

δ_H (ppm)	(A) → 4)-3-*O*-Me-β-D-Glc*p*A-(1 →	(B) → 6)-4-*O*-Me-α-D-Glc*p*-(1 →
H1	4.53	5.35
H2	3.50	3.50
H3	3.56	3.75
H4	3.85	3.41
H5	3.93	3.75
$H6_R$	–	3.84
$H6_S$	–	4.06
*O*Me	3.64	3.56

Table 2. $^{3}J_{H,H}$ coupling constants (in Hz) for **1**.

$^{3}J_{H,H}$ (Hz)	(A) → 4)-3-*O*-Me-β-D-Glc*p*A-(1 →	(B) → 6)-4-*O*-Me-α-D-Glc*p*-(1 →
1,2	7.3	3.9
2,3	ND	10.0
3,4	ND	9.7
4,5	8.8	9.6
$5,6_R$	–	< 3
$5,6_S$	–	< 3
$6_R,6_S$	–	− 11.1

$H6_R$(B) at δ_H 3.84 ppm and both the methyl groups at δ_H 3.56 (Me(B)) and H4(B) (δ_H 3.41 ppm) are in agreement with this assignment.

Figure 2 shows a 500 MHz NOESY spectrum of **1**. All peaks were positive, and the normalized intensities of well-resolved cross peaks are indicated in Table 3. It can

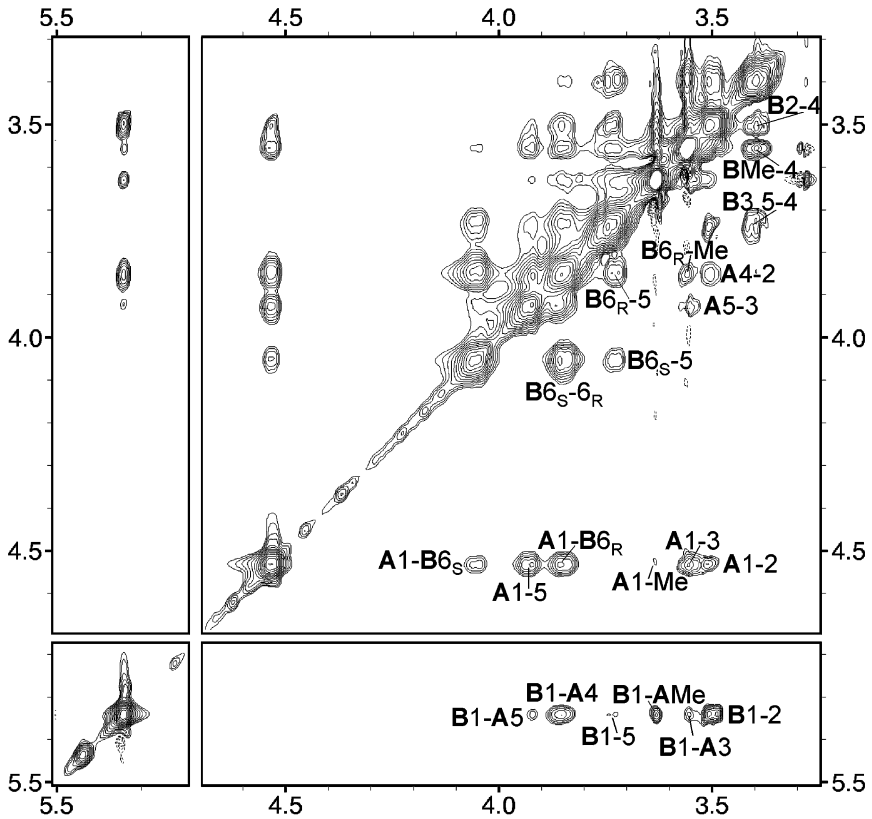

Figure 2. 500 MHz NOESY spectrum of **1** at 303 K (mixing time, 100 ms).

Marcel Dekker, Inc.
270 Madison Avenue, New York, New York 10016

Table 3. Experimental and calculated NOESY normalized intensities.

Cross peak	Exp. norm. intensity (%)	Calcd norm. intensity (%)	Cross peak	Exp. norm. intensity (%)	Calcd norm. intensity (%)[c]
H1/H2(A)[a]	3.5	1.9	H1/H2(B)	7.6	7.7 (7.7)
H1/H3(A)[a]	6.0	4.2	H1/H5(B)	1.1	0.7 (0.7)
H1/H5(A)	8.8	8.9	H1(B)/H3(A)	1.5[a]	1.1 (1.3)
H1(A)/H6$_S$(B)	4.2	5.0	H1(B)/H4(A)	6.8	6.5 (6.8)
H1(A)/H6$_R$(B)[b]	10.6	9.1	H1(B)/H5(A)	1.2	0.0 (1.0)
H4/H2(A)	4.9	4.3	H1(B)/Me(A)	2.5	3.1 (2.6)
H6$_S$/H6$_R$(B)	33.1	33.1[d]			
H6$_S$/H5(B)	6.8	6.8[d]			
H6$_R$/H5(B)	8.3	8.4[d]			

[a]Partially overlapped peaks.
[b]H6$_R$(B) and H4(A) are overlapped. Calculated intensity for H1/H4(A) (0.6) was added.
[c]Calculated values for a population of 85:10:5 of minima ($\omega_B gg$) in brackets.
[d]Calculated intensities were renormalized according to the experimental value of H6$_S$/H6$_R$(B).

be seen that a good match is observed between the experimental data and those estimated through molecular mechanics simulations (see below).

The chemical shifts and coupling constants correspond to a $^4C_1$ conformation for both pyranose rings. In addition, the coupling constants $^3J_{5,6S}$ and $^3J_{5,6R}$ (both less than 3 Hz) indicate a high population of the *gg* conformer for the glycosyloxymethyl group in residue B. The weak NOESY cross peak between protons H4(B) and H6$_R$(B) also points to a significant proportion of this rotamer. The *gg*:*gt* ratio in other α- and β-(1 → 6)-linked oligo- and polysaccharides ranges from 60:40 to 75:25 (25–28), or reaches about 40:60 when maximum entropy analysis is applied.[13] The coupling constant H5/H6$_R$ usually ranges from 4 Hz to 6 Hz in these cases, whereas H5/H6$_S$ ranges between 1.5 Hz and 4.5 Hz. The value of $^3J_{5,6R}$ includes information about the proportion of the *gt* rotamer. Apparently, this rotamer is relatively disfavored in B33 polysaccharide. Small $J_{5,6S}$ and $J_{5,6R}$ (less than 2 Hz) have been observed in another polysaccharide having the fragment β-D-Glc*p*A-(1 → 6)-α-D-Glc*p*-(1 → (29). Analogously, very narrow peaks are observed for both methylene protons in a polysaccharide having the repeating unit → 6)-β-D-Glc*p*-(1 → .[27] However, the preponderance of the *gg* rotamer does not depend exclusively on the β-(1 → 6) linkage, as a $^3J_{5,6R}$ of 6 Hz is found in gentiobiose[13] and related oligosaccharides.[25]

NOE can also provide information about the orientation of methyl groups in B33 polysaccharide. The local correlation time of this flexible group and overlapping make a full-relaxation-matrix-based analysis difficult, although qualitative results can be derived from NOESY spectra. In the case of Me(A), H2(A)/Me(A), and H4(A)/Me(A), cross-peak intensities are similar, indicating that this group is placed at a comparable distance from both protons in the time-averaged conformation. In fact, the best energy orientation, according to our molecular modeling (see below), has a γ_A angle close to 270°. Interestingly, the Me(A)/H1(B) NOESY cross peak indicates that the orientation of the glycosidic linkage approaches both groups, which agrees with our molecular modeling results. In the case of Me(B), the Me(B)/H6$_R$(B) NOESY cross peak gives additional evidence of the preferred *gg* orientation of the glycosyloxymethyl group. It

Marcel Dekker, Inc.
270 Madison Avenue, New York, New York 10016

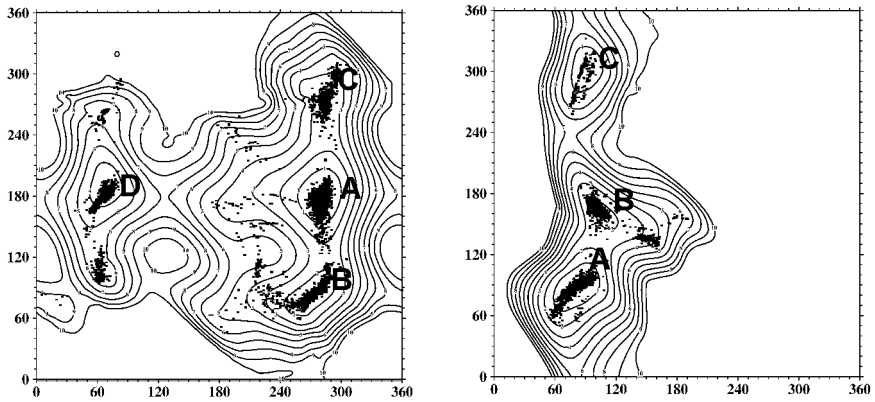

Figure 3. Adiabatic maps calculated with MM3(92) for disaccharides AB and BA, and minima found with the CICADA procedure for the tetrasaccharide ABAB.

also indicates that in the time-averaged orientation, the methyl group is located close to H4(B), $H6_R$(B), and—probably—H5(B). The overlapping of H3(B) and H5(B) does not allow further information.

Molecular Modeling

As a first step to determining the overall three-dimensional structure of the polysaccharide, information on the amount of accessible conformational space was obtained through molecular mechanics calculations. Relaxed and adiabatic maps were calculated for the disaccharides AB and BA. Eight possible starting structures were obtained by combining the orientations of secondary hydroxyl groups (*c* or *r*) and the torsion angle ω_B (*gg* or *gt*); the resulting relaxed maps were combined to generate the adiabatic maps (Figure 3, Table 4).

Table 4. Glycosidic torsion angles and relative energy for minima found by molecular mechanics calculations for the AB and BA disaccharides.

		$\omega_B gt$			$\omega_B gg$		
Disaccharide	Minima	Φ (°)	Ψ (°)	ΔE (kcal/mol)	Φ (°)	Ψ (°)	ΔE (kcal/mol)
AB	I	278.7	176.6	0.00	278.4	176.8	0.26
	II	278.8	87.5	1.53	269.80	79.0	1.76
	III	275.2	275.0	1.89	–	–	–
	IV	67.5	192.2	3.35	67.1	192.5	3.44
BA	I	81.5	89.3	0.00	80.8	90.3	0.42
	II	110.0	159.5	1.74	101.2	158.9	2.10
	III	96.5	305.8	3.45	89.4	301.8	3.15

Marcel Dekker, Inc.
270 Madison Avenue, New York, New York 10016

It can be observed that the populated region for the β-(1 → 6) linkage is fairly extended, mainly around Ψ_A. This property is independent of the *gg* or *gt* orientation of the lateral chain of the glucose moiety, even though the orientation *gt* leads to a minimum at $(\Phi_A,\Psi_A) = (275.2°, 275.0°)$ that is not found when ω_B is *gg*. The molecular mechanics calculations indicate that the *gt* orientation is more favorable than the *gg* one for ω_B (from 0.26 to 0.09 kcal/mol). However, it has been shown that MM3 calculations overestimate the population of the *gt* rotamers,[14,28] so both orientations were considered in all minima. The torsion angle (Φ_A,Ψ_A) maps indicate two different conformational families. The most populated one is centered at $\Phi_A = 275°$, in agreement with the *exo*-anomeric effect;[29] Ψ_A, ranging from 80° to 300°, is very extended, but a value close to 180° seems the most favorable. A second family corresponds to $\Phi_A = 80°$. Although less extended around Ψ_A, it is again centered at $\Psi_A = 180°$. A counter-clockwise (*r*) orientation of the secondary hydroxyl groups was found in all minima for both monomers.

The disaccharide BA presents a low-energy region centered at $\Phi_B = 90°$, in agreement with the *exo*-anomeric effect, and extended along Ψ_B. The global minimum corresponds to $(\Phi_B,\Psi_B) = (80.8°, 90.3°)$, with two other minima appearing at $\Psi_B = 180°$ and $\Psi_B = 300°$, within an energy window of 10 kcal/mol. As in the previous disaccharide, the calculated energy for *gt* rotamers is less than that for *gg* rotamers (about 0.4 kcal/mol), except for minimum III. Again, a counterclockwise orientation (*r*) is found in most cases. In addition, it was found that the geometry of the glycosidic linkage corresponding to the global energy minimum was little influenced by the value of ω_B.

Besides the knowledge gained from the adiabatic maps obtained from grid searching, the inter-residue linkages were studied with the CICADA algorithm for conformational searches.[16] Initially, a fast search was carried out on disaccharides AB and BA: torsion angles Φ_A, Ψ_A, Φ_B, Ψ_B, ω_A, ω_B, γ_A, and γ_B were systematically modified using an incremental step set to 50°. About 3700 (AB) and 3300 (BA) minima were found and grouped into families according to their torsion angles. In the case of disaccharide AB, low-energy families had (Φ_A,Ψ_A) values close to (280°, 180°), in agreement with the global minimum found in the adiabatic map. A distribution of three rotamers was found for the ω_B torsion angle, *gt* and *gg* being those present in the two lowest-energy families. In the case of disaccharide BA, all low-energy families had (Φ_B,Ψ_B) values corresponding to the global minimum found in the adiabatic map (80°, 90°). For both disaccharides, the ω_A torsion angle was close to 125° in most low-energy minima, and the methyl groups had the *r* orientations ($\gamma_A \sim 265°$, $\gamma_B \sim 100°$).

In order to evaluate the behavior of glycosidic torsion angles in the polysaccharide, an ABAB tetrasaccharide was built and submitted to a CICADA study. The starting geometry corresponded to the global minima found for the corresponding disaccharides. All the torsion angles Φ_A, Ψ_A, Φ_B, Ψ_B, and ω_B, involved in the sequence were driven at an increment of 25°. Nine thousand minima were found and grouped into families, as presented in Figure 3. It can be observed that the minima found with CICADA match the energy maps well. The linkages adopt an orientation very similar to that found in the disaccharides, and no significant reduction of the conformational space due to the glycosidation was detected. Moreover, no minimum having an energy lower than that of the starting structure was found.

The conformations arising from molecular mechanics simulations were used to calculate the NOESY intensities through the complete relaxation matrix. Isotropic

MARCEL DEKKER, INC.
270 Madison Avenue, New York, New York 10016

motion and external relaxation of 0.1 s^{-1} were assumed in the calculation.[24] Since NOEs are dependent on the correlation time (τ_c), different values were used in order to obtain the best match between experimental and calculated NOEs for the H1(A)/H5(A) and H1(B)/H2(B) pairs. A τ_c of 2.8 ns gave the best match in both cases (Table 3). In a first approximation, intensities were calculated from the global minima found for disaccharides AB and BA. Orientation around the AB linkage has a great influence on the intensities of NOESY cross peaks involving H1(A), H5(B), and the methylene protons $H6_{R,S}$(B). The relative intensities of peaks $H6_S$(B)/H5 and $H6_R$(B)/H5 can be used to estimate the population around ω_B. Thus, for a *gt* rotamer, an $H6_S$-5/$H6_R$-5 ratio of around 2:1 has been calculated. In this orientation, protons H5(B) and $H6_S$(B) adopt a *gauche* orientation, whereas H5(B) and $H6_R$(B) are *trans*. A ratio of approximately 1:1 is found for the *gg* rotamer, as both H6(B) are *gauche* relative to H5 in this orientation. Experimentally, a ratio of 0.8:1 is found, which agrees with the low values for $^3J_{H5,H6R}$ and $^3J_{H5,H6S}$ and indicates a very high population of the *gg* rotamer. The calculated normalized intensities for $H6_S$/H5, $H6_R$/H5, and $H6_S$/$H6_R$ (8.6, 10.6, and 42.1, respectively) were higher than the experimental ones (6.8, 8.3, and 33.1). However, when relative intensities of $H6_S$/$H6_R$ cross peaks were plotted against mixing time, no linearity was found, probably due to the strong geminal coupling and the local flexibility. Calculated intensities for cross peaks $H6_S$/H5 and $H6_R$/H5 were renormalized (multiplied by 0.79) as required to get an intensity of 33.1 for $H6_S$/$H6_R$, resulting in an excellent match with experimental intensities.

Regarding the (Φ_A,Ψ_A) glycosidic torsion angles, experimental NOESY signals for H1(A)/$H6_R$(B) are about 2.5-fold more intense than the H1(A)/$H6_S$(B) signals. The values calculated from the global energy minimum conformation agree with a higher intensity for H1(A)/$H6_R$(B), although the difference in intensity was smaller (ratio 1.8), even when the overlapping of cross peaks H1(A)/H4(A) and H1(A)/$H6_R$(B) was considered.

Orientation around the B → A linkage modifies mainly the intensities of the NOESY cross peaks H1(B)/H3(A), H1(B)/H4(A), and H1(B)/H5(A). The H1(B)/H4(A) NOESY intensities—calculated from the global energy minimum conformation—agree with a close position of these protons. However, higher intensities than those calculated are observed for H1(B)/H3(A) (whose integral is difficult to calculate because of partial overlapping), as is also the case for the H1(B)/H5(A) cross peak. The presence of the latter was not expected for the global minimum, but was predicted for minimum III (for which the calculated distances for H1(B)/H3(A) and H1(B)/H5(A) are 2.5 Å and 2.1 Å, respectively). A good match is found when an 85:10:5 distribution of minima I, II, and III is used to calculate the intensities (Table 3).

Molecular mechanics were also applied for disaccharides lacking the methyl group close to the linkage position (that is, without 4-*O*-Me in AB and without 3-*O*-Me in BA), to evaluate the possible additional stiffness due to the presence of these substituents. Table 5 shows the relative energies between minima calculated for methylated (AB and BA) or non-methylated disaccharides (AB′ and BA′). It can be seen that differences between global energy minima corresponding to the *gg* and *gt* rotamers are lower for the natural disaccharide than for the non-methylated model (ΔE_{gg-gt} = 0.53 kcal/mol in AB′ and 0.26 kcal/mol in AB). Consequently, a higher proportion of *gg* rotamer is expected in the former case. Certain 4,6-linked oligosaccharides have been described[25] with a *gg*:*gt* ratio from 60:40 to 75:25 depending

Marcel Dekker, Inc.
270 Madison Avenue, New York, New York 10016

Table 5. Differences in energy between *gt* and *gg* rotamers found for minima calculated for methylated (AB and BA) or non-methylated disaccharides (AB′ and BA′).

Minima		ΔE(*gt*−*gg*) (kcal/mol)		ΔE(*gt*−*gg*) (kcal/mol)
A	AB	−0.26	AB′	−0.53
B		−0.23		−0.42
C		–		–
D		−0.09		−0.57
A	BA	−0.42	BA′	−0.45
B		−0.36		−0.25
C		0.30		−0.25

on the orientation of the substituent at O-4. However, this explanation is not applicable to other polysaccharides having very small $^3J_{5,6}$.[27,30]

Conformational Properties of Polymer Chains

Theoretically, conformational characteristics can be calculated from statistical ensembles of disordered chains using molecular mechanics.[17] Polymer chain models with corresponding descriptors have been presented for different polysaccharides,[12] and this approach has been used in the present study to simulate the conformational properties of **1**. The extension of the chain in a preferred direction can be considered as a descriptor of its stiffness. Disordered chains were generated from the AB and BA disaccharides using the corresponding (Φ,Ψ) maps, and persistence lengths (L_p) were calculated from the resulting statistical ensembles. The torsion angle ω_B was distributed at different ratios between the values found for the *gg* and *gt* conformers. The results are shown in Figure 4. An asymptotic behavior was reached for polymers comprising

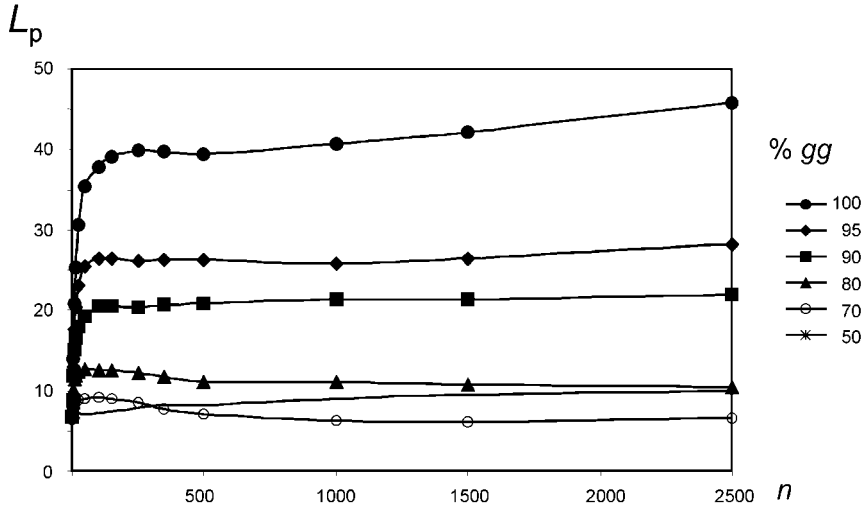

Figure 4. Calculated L_p vs. number of repeating units at different ratios of *gg* rotamers.

MARCEL DEKKER, INC.
270 Madison Avenue, New York, New York 10016

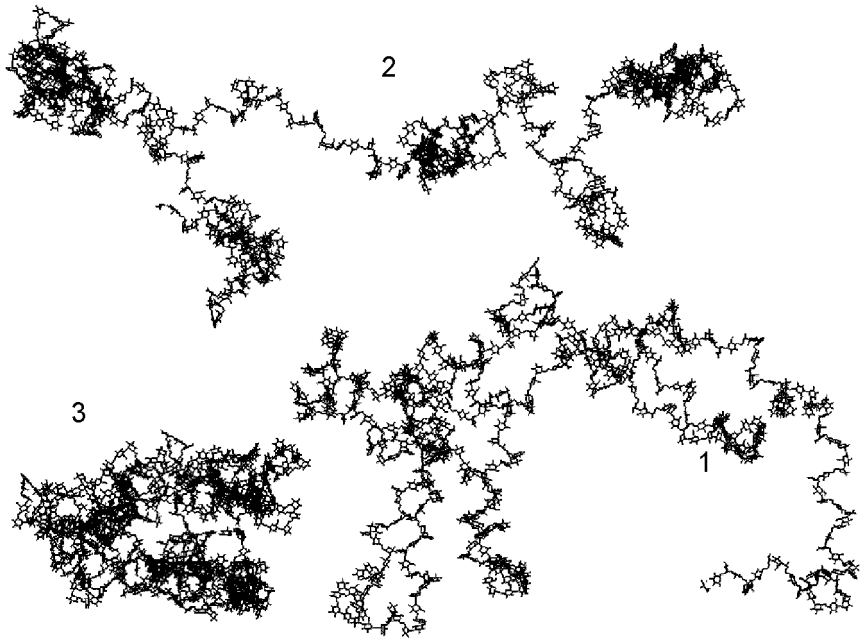

Figure 5. Snapshots of randomly generated chains from METROPOL corresponding to 1) 95%, 2) 80%, and 3) 50% of *gg* rotamers. Each chain contains 500 residues (250 repeating units).

between 250 and 400 repeating units at 298 K. In all cases, the depictions of chains indicate their flexible behavior. Moreover, the flexibility increases with the population of *gt* conformers, without any preferred direction when the *gg*:*gt* ratio is less than 1:1. Figure 5 shows snapshots of the simulation. Zones with a helical orientation interspersed with crowed regions can be observed. The increase in the percentage of *gt* rotamer diminishes the helical zones, to the point of resulting in an overcrowded globular chain when the ratio is 1:1 (Figure 5.3). As the algorithm does not take into account the existence of steric interactions between non-adjacent residues, the modeled chains cannot be reoriented to avoid such interactions. Thus, the result is only estimative. However, it is reasonable to think that there would be fewer intramolecular close contacts with a low proportion of *gt* rotamer, as is found experimentally. This could be an additional factor for the low ratio of the *gt* rotamer in this polysaccharide.

CONCLUSIONS

This work presents the study of the three-dimensional structure of a capsular polysaccharide isolated from strain B33, a fast-growing soybean-nodulating bacterium that most probably belongs to the species *Sinorhizobium fredii* or *Sinorhizobium xinjiangense*. A time-averaged conformation can be deduced from NMR data. Thus, coupling constants indicate that both pyranose rings are essentially $^4C_1$, with a preferred *gg* orientation for the glycosyloxymethyl group in β-(1 → 6) linkage. NOE data corroborate this orientation. Additionally, they indicate that the orientation of glycosidic torsion angles in α-(1 → 4) and β-(1 → 6) linkages agree with the exo-anomeric effect.

Models were built using the molecular mechanics force field MM3(92). A very good match was found when they were used in a full relaxation matrix simulation of the experimental NOESY spectra. In the case of the α-(1 → 4) linkage, other minima besides the global minimum must exist in solution to explain the NOE intensities. An 85:10:5 distribution of minima leads to the best match. In the case of the β-(1 → 6) linkage, MM3 fails to predict a distribution of minima for the glycosyloxymethyl in the glucose moiety. The model is too simple, and it is generally recognized that the preference for *gauche* orientations is a solvent-dependent phenomenon.[31] Nevertheless, the NOESY simulation was good when only the *gg* rotamer was used.

In order to estimate the influence of the neighboring methyl group, disaccharides without these groups were built and studied by molecular modeling. The results indicate that substitution on O-4 leads to a small relative destabilization of the *gt* rotamer for the β-(1 → 6) linkage. When a simulation is made of the conformational properties of polymer chains, it has been observed that the chain flexibility grows with the proportion of *gt* rotamer, together with the number of close contacts. This could be an additional factor in explaining the high proportion of rotamer *gg*.

Finally, computational results show that there is an important amount of conformational freedom for the glycosidic torsion angles of the AB and BA disaccharides. It is hypothesized from these data that the nature of the receptor binding sites can easily modulate the conformational behavior of the polysaccharide.

ACKNOWLEDGMENTS

We thank the Comisión Interministerial de Ciencia y Tecnología (grant no. BIO099-0614-C03-01 and 02) and INCO-DC ERBIG18GT970191 for financial support. Thanks are extended to Dr. J.E. Ruiz Sainz (Departamento de Microbiología, Facultad de Biología, Universidad de Sevilla) for supplying bacterial cultures.

REFERENCES

1. Van Berkum, P.; Eardy, B.D. Molecular evolutionary systematic of the *Rhizobiaceae*. In *The Rhizobiaceae*; Spaink, H.P., Kondorosi, A., Hooykaas, P.J.J., Eds.; Kluwer Academic Publishers: Dordrecht, The Netherlands, 1998; 1–24.
2. Day, B.R.; Loh, J.T.; Cohn, J.; Stacey, G. Signal exchange involved in the establishment of the *Bradyrhizobium* legume symbiosis. In *Prokaryotic Nitrogen Fixation. A Model System for the Analysis of a Biological Process*; Triplett, E.W., Ed.; Horizon Scientific Press: Norfolk, England, 2000; 385–415.
3. Kannenberg, E.L.; Reuhs, B.L.; Fosberg, L.S.; Carlson, R.W. Lipopolysaccharide and K-antigens: their structures, biosynthesis and functions. In *The Rhizobiaceae*; Spaink, H.P., Kondorosi, A., Hooykaas, P.J.J., Eds.; Kluwer Academic Publishers: Dordrecht, The Netherlands, 1998; 119–154.
4. Becker, A.; Pühler, A. Production of exopolysaccharides. In *The Rhizobiaceae*; Spaink, H.P., Kondorosi, A., Hooykaas, P.J.J., Eds.; Kluwer Academic Publishers: Dordrecht, The Netherlands, 1998; 97–118.
5. Rodriguez-Carvajal, M.A.; Tejero-Mateo, P.; Espartero, J.L.; Ruiz-Sainz, J.E.; Buendia-Claveria, A.M.; Ollero, F.J.; Yang, S.S.; Gil-Serrano, A.M. Determination

of the chemical structure of the capsular polysaccharide of strain B33, a fast-growing soya bean-nodulating bacterium isolated from an arid region of China. Biochem. J. **2001**, *357* (2), 505–511.
6. Rutherford, T.J.; Spackman, D.G.; Simpson, P.J.; Homans, S.W. 5 Nanosecond molecular dynamics and NMR study of conformational transitions in the sialyl-Lewis X antigen. Glycobiology **1994**, *4* (1), 59–68.
7. Poveda, A.; Asensio, J.L.; Martin-Pastor, M.; Jimenez-Barbero, J. Exploration of the conformational flexibility of the LeX related oligosaccharide GalNAcα(1 → 3)-Galβ(1 → 4)(Fucα(1-)3) → Glc by ^{1}H NMR relaxation measurements and molecular dynamics simulations. J. Chem. Soc., Chem. Commun. **1996**, *3*, 421–422.
8. IUPAC-IUB. Commission of Biochemical Nomenclature. Arch. Biochem. Biophys. **1971**, *145*, 405–621.
9. Allinger, N.L.; Yuh, Y.H.; Lii, J.-H. Molecular mechanics. The MM3 force field for hydrocarbons. J. Am. Chem. Soc. **1989**, *111*, 8551–8566.
10. Allinger, N.L.; Rahman, M.; Lii, J.-H. A molecular mechanics force field (MM3) for alcohols and ethers. J. Am. Chem. Soc. **1990**, *112*, 8293–8307.
11. Allinger, N.L.; Zhu, Z.-Q.; Chen, K. Molecular mechanics (MM3) studies of carboxylic acids and esters. J. Am. Chem. Soc. **1990**, *112*, 6120–6133.
12. Braccini, I.; Grasso, R.P.; Perez, S. Conformational and configurational features of acidic polysaccharides and their interactions with calcium ions: a molecular modeling investigation. Carbohydr. Res. **1999**, *317* (1–4), 119–130.
13. Poppe, L. Modeling carbohydrate conformations from NMR data: maximum entropy rotameric distribution about the C5–C6 bond in gentiobiose. J. Am. Chem. Soc. **1993**, *115*, 8421–8426.
14. Asensio, J.L.; Canada, F.J.; Jimenez-Barbero, J. Studies of the bound conformations of methyl alpha-lactoside and methyl beta-allolactoside to ricin B chain using transferred NOE experiments in the laboratory and rotating frames, assisted by molecular mechanics and dynamics calculations. Eur. J. Biochem. **1995**, *233* (2), 618–630.
15. Preusser, A. Algorithm 671—FARB-E-2D: fill area with bicubics on rectangles—a contour plot program. ACM Trans. Math. Softw. **1989**, *15* (1), 79–89.
16. Koca, J.; Perez, S.; Imberty, A. Conformational analysis and flexibility of carbohydrates using the CICADA approach with MM3. J. Comput. Chem. **1995**, *16* (3), 296–310.
17. Boutherin, B.; Mazeau, K.; Tvaroska, I. Conformational statistics of pectin substances in solution by a Metropolis Monte Carlo study. Carbohydr. Polym. **1997**, *31*, 1–12.
18. Metropolis, N.; Rosenbluth, A.W.; Rosenbluth, M.M.; Teller, A.H.; Teller, E. Equation of state calculations by fast computing machines. J. Chem. Phys. **1953**, *21*, 1087–1092.
19. Lapasin, R.; Pricl, S. *Rheology of Industrial Polysaccharides, Theory and Applications*; Blackie Academic and Professional: London, 1995; 622.
20. Parella, T.; Sánchez-Ferrando, F.; Virgili, A.J.M.R. Improved sensitivity in gradient-based 1D and 2D multiplicity-edited HSQC experiments. J. Magn. Reson. **1997**, *126*, 274–277.
21. Kumar, A.; Ernst, R.R.; Wuthrich, K. A two-dimensional nuclear Overhauser enhancement (2D NOE) experiment for the elucidation of complete proton–proton

Marcel Dekker, Inc.
270 Madison Avenue, New York, New York 10016

cross-relaxation networks in biological macromolecules. Biochem. Biophys. Res. Commun. **1980**, *95* (1), 1–6.
22. Goddard, T.D.; Kneller, D.G. *SPARKY, 3.1*; University of California: San Francisco, 2002.
23. Neuhaus, D.; Williamson, M.P. *The Nuclear Overhauser Effect: Chemical Applications*; VCH Publishers: New York, 1989; 522.
24. Pastor, M.M. *Estructura y Dinámica de Oligosacáridos Mediante RMN y Cálculos de Mecánica y Dinámica Molecular*; Universidad Autonoma de Madrid: Madrid, 1997.
25. Nishida, O.; Hiroshi, H.; Hiroshi, O.; Meguro, H.; Zushi, S.; Uzawa, J.; Ogawa, T. Syntheses and 1H-NMR studies of methyl 4,6-di-*O*-glucopyranosyl-β-D-glucopyranosides chirally duterated at the (1 → 6) linkage moiety. Agric. Biol. Chem. **1988**, *52* (4), 1003–1011.
26. Ohrui, H.; Nishida, Y.; Watanbe, M.; Hori, H.; Meguro, H. 1H-NMR Studies on (6R)- and (6S)-deuterated (1-6)-linked disaccharides: assignment of the preferred rotamers about C5–C6 bond of (1 → 6)-disaccharides in solution. Tetrahedron Lett. **1985**, *26* (27), 3251–3254.
27. Monteiro, M.A.; Slavic, D.; St. Michael, F.; Brisson, J.R.; MacInnes, J.I.; Perry, M.B. The first description of a (1 → 6)-beta-D-glucan in prokaryotes: (1 → 6)-beta-D-glucan is a common component of *Actinobacillus suis* and is the basis for a serotyping system. Carbohydr. Res. **2000**, *329* (1), 121–130.
28. Dowd, M.K.; Reilly, P.J.; French, A.D. Relaxed-residue conformational mapping of the three linkage bonds of isomaltose and gentiobiose with MM3(92). Biopolymers **1994**, *34* (5), 625–638.
29. Tvaroska, I.; Bleha, T. Anomeric and exo-anomeric effects in carbohydrate chemistry. Adv. Carbohydr. Chem. Biochem. **1989**, *47*, 45–123.
30. Robijn, G.W.; Gutierrez Gallego, R.; van den Berg, D.J.; Haas, H.; Kamerling, J.P.; Vliegenthart, J.F. Structural characterization of the exopolysaccharide produced by *Lactobacillus acidophilus* LMG9433. Carbohydr. Res. **1996**, *288*, 203–218.
31. Kirschner, K.N.; Woods, R.J. Solvent interactions determine carbohydrate conformation. Proc. Natl. Acad. Sci. U. S. A. **2001**, *98* (19), 10541–10545.

Received January 29, 2003
Accepted August 13, 2003

MARCEL DEKKER, INC.
270 Madison Avenue, New York, New York 10016